Report

A Novel Form of Motility in Filopodia Revealed by Imaging Myosin-X at the Single-Molecule Level

Michael L. Kerber,[1,2] Damon T. Jacobs,[1,2]
Luke Campagnola,[1] Brian D. Dunn,[1] Taofei Yin,[1]
Aurea D. Sousa,[1,3] Omar A. Quintero,[1,4]
and Richard E. Cheney[1,*]
[1]Department of Cell and Molecular Physiology
School of Medicine
University of North Carolina at Chapel Hill
Chapel Hill, NC 27599
USA

Summary

Although many proteins, receptors, and viruses are transported rearward along filopodia by retrograde actin flow [1–3], it is less clear how molecules move forward in filopodia. Myosin-X (Myo10) is an actin-based motor hypothesized to use its motor activity to move forward along actin filaments to the tips of filopodia [4]. Here we use a sensitive total internal reflection fluorescence (TIRF) microscopy system to directly visualize the movements of GFP-Myo10. This reveals a novel form of motility at or near the single-molecule level in living cells wherein extremely faint particles of Myo10 move in a rapid and directed fashion toward the filopodial tip. These fast forward movements occur at ~600 nm/s over distances of up to ~10 μm and require Myo10 motor activity and actin filaments. As expected for imaging at the single-molecule level, the faint particles of GFP-Myo10 are diffraction limited, have an intensity range similar to single GFP molecules, and exhibit stepwise bleaching. Faint particles of GFP-Myo5a can also move toward the filopodial tip, but at a slower characteristic velocity of ~250 nm/s. Similar movements were not detected with GFP-Myo1a, indicating that not all myosins are capable of intrafilopodial motility. These data indicate the existence of a novel system of long-range transport based on the rapid movement of myosin molecules along filopodial actin filaments.

Results and Discussion

Filopodia are slender actin-based extensions thought to function as cellular sensors in processes such as nerve growth and blood vessel development. Filopodia have a relatively simple structure consisting of a bundle of parallel actin filaments surrounded by the plasma membrane [5, 6]. Each actin filament has its barbed end oriented toward the tip of the filopodium, and actin monomers are constantly added to the filament at its barbed end. The actin in filopodia typically moves rearward at rates of 10–100 nm/s in a process known as retrograde flow. Although retrograde flow [7] is now known to be powered by a combination of actin polymerization and myosin-II-mediated contraction [8], the mechanisms by which molecules move forward in filopodia are much less clear. Microtubules and membranous vesicles are generally absent from filopodia, so forward movement in filopodia is likely to depend either on diffusion or on an actin-based mechanism.

Myo10 is an actin-based motor protein that localizes to the tips of filopodia and has potent filopodia-inducing activity [9, 10]. The Myo10 heavy chain consists of a myosin head domain responsible for force production, a neck domain that provides binding sites for calmodulin or calmodulin-like light chains [11], and a large tail [9]. The tail includes a segment that was initially predicted to form a coiled coil [12], although the oligomerization status of Myo10 is currently unclear [13, 14]. The remainder of the tail has been reported to bind to PIP_3 [15], microtubules [16], and β-integrins [17]. Imaging with conventional epifluorescence revealed that the bright puncta of GFP-Myo10 normally present at the tips of filopodia sometimes move slowly rearward at 10–20 nm/s [4], the rate of retrograde actin flow in HeLa filopodia. Bright puncta also occasionally moved forward at ~80 nm/s, leading to the hypothesis that Myo10 moves forward by using its barbed-end motor activity to transport itself along filopodial actin filaments. Consistent with this, a Myo10 construct comprised only of the head, neck, and predicted coiled coil (Myo10-HMM) was sufficient for tip localization [4]. Kinetic analyses of Myo10 head-neck constructs indicate that they have duty ratios intermediate between those of highly processive motors, such as Myo5a, and nonprocessive motors, such as muscle myosin [18, 19]. Most importantly, recent single-molecule experiments with in vitro motility assays show that a HMM-like Myo10 forced dimer can move rapidly and processively on artificial actin bundles at 340–780 nm/s [20].

To test whether living cells exhibit robust but previously unsuspected forms of trafficking at the single-molecule level, here we use TIRF microscopy to image the movements of GFP-tagged motor proteins in filopodia. TIRF provides high sensitivity whereas the linear organization and defined polarity of filopodia greatly facilitates particle tracking and analysis. In addition, the ~100 nm thickness of a filopodium means that all or most of a filopodium will be within the 100–200 nm penetration distance of the TIRF field. Imaging substrate-attached filopodia with TIRF thus provides a system that has much of the simplicity of an in vitro motility assay, but in the context of a living cell.

TIRF Reveals a Novel Form of Rapid Motility in Filopodia

To test the sensitivity of our TIRF system, we adsorbed low concentrations of pure GFP onto coverslips and imaged with TIRF. As expected for single-molecule imaging of GFP [21], this resulted in the detection of faint spots that were diffraction limited, underwent stepwise bleaching, and exhibited "blinking" (Movie S1 available online). When living HeLa cells were transiently transfected with full-length GFP-Myo10 and imaged by TIRF under the same conditions, bright labeling was observed at the tips of filopodia as well as at the ventral surface of the cell (Movie S2). Most importantly, close inspection of individual filopodia revealed a novel form of motility in

*Correspondence: cheneyr@med.unc.edu
[2]These authors contributed equally to this work
[3]Present address: National Institutes of Health, NIDCD, Bethesda, MD 20892, USA
[4]Present address: Department of Cellular and Molecular Physiology, Pennsylvania State University, College of Medicine, Hershey, PA 17033, USA
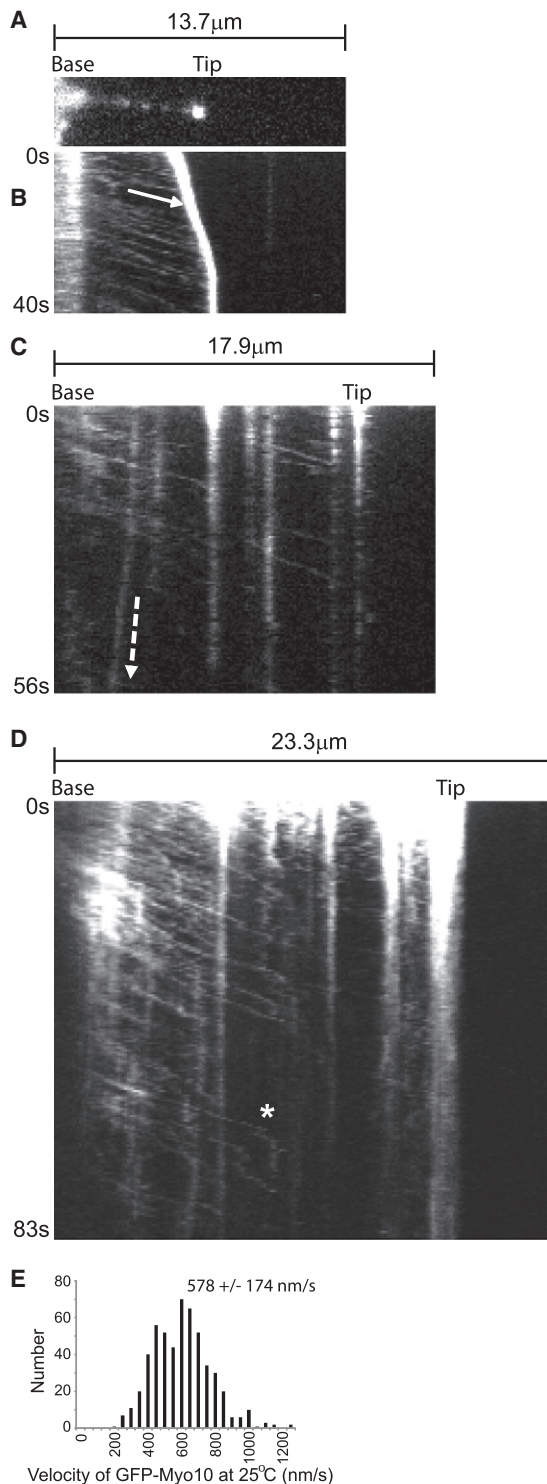
Figure 1. TIRF Microscopy Reveals Fast Forward Movements of Faint Particles of GFP-Myo10 in Living Cells

(A) TIRF image of a single filopodium from a HeLa cell expressing GFP-Myo10 showing a bright punctum of GFP-Myo10 at the tip of the filopodium, several faint particles of GFP-Myo10 along the shaft, and diffuse fluorescence at the base of the filopodium (see Movie S3).

(B) Kymograph generated from time-lapse imaging of the same filopodium revealing numerous faint tracks (arrow) sloping gently down to the right that correspond to rapid movements of faint particles toward the tip. The very bright track corresponds to the tip of the filopodium, which was initially

which extremely faint particles of GFP-Myo10 moved rapidly toward the tip (Movies S3 and S4).

The movements of the faint particles along a given filopodium are clearly illustrated in kymographs, which reveal numerous faint tracks corresponding to the rapid and directed movements of faint particles of GFP-Myo10 toward the tip (Figure 1; Figure S1). Approximately a dozen such tracks are visible in the 40 s time lapse illustrated in Figure 1B. Tracks from these fast forward movements appeared to have relatively constant intensities and most traveled the entire ~5 μm length of the filopodium. Although most particles moved in a smooth and apparently processive fashion until they reached the filopodial tip, particles occasionally paused or transiently reversed, generating Z-shaped tracks (Figure 1D; Figure S1). Rapid forward movements of faint Myo10 particles were detected under a variety of TIRF imaging conditions, including the use of different camera settings, different magnifications, and a different TIRF illuminator (Figure S1). At 25°C, the faint particles of Myo10 moved forward at an average velocity of 578 ± 174 nm/s (Figure 1E). At 37°C, the particles moved faster (840 ± 210 nm/s), as expected for a motor-driven biological process. The velocities of GFP-Myo10 particles detected here in living cells are quite similar to the 340–780 nm/s reported for movements of individual molecules of a Myo10 forced-dimer on artificial actin bundles [20]. The forward movements detected here by TIRF are clearly distinct from the relatively infrequent forward movements of bright GFP-Myo10 puncta detected previously by conventional fluorescence in that the particles detected here are much fainter, move 5- to 10-fold faster, and move forward much more frequently.

In addition to the fast forward movements of faint particles of Myo10, we also detected slow rearward movements (Figure 1C; Figure S1). The average rate of the rearward movements was 23 ± 8 nm/s (137 measurements from 20 filopodia), a velocity consistent with the hypothesis that GFP-Myo10 moves rearward by binding to actin filaments undergoing retrograde flow. The bright puncta of GFP-Myo10 at the tips of filopodia were generally stationary and thus generated bright vertical tracks that became gradually dimmer because of photobleaching. Vertical tracks were also sometimes present at different points along a filopodium, indicating that some Myo10 molecules within the filopodial shaft are stationary, perhaps because of association with integrin-based adhesions [17].

It should be noted that we observed obvious movement of Myo10 particles in slender extensions that extended forward during imaging and that would thus be functionally defined as filopodia (Figures 1A and 1B). We also observed similar movements in slender extensions that had the branched morphology

extending forward at ~100 nm/s and then stopped. The faint vertical track beyond the tip corresponds to a faint particle of fluorescent debris.

(C) Kymograph from a branched retraction fiber in a HeLa cell stably expressing GFP-Myo10. This kymograph shows faint tracks from fast forward movements as well as vertical tracks from stationary particles. One track slopes steeply down to the left and corresponds to GFP-Myo10 that was moving slowly rearward (dashed arrow).

(D) Kymograph from a HeLa cell expressing GFP-Myo10 showing numerous faint tracks that terminate midway along a filopodium. One particle moved rapidly forward, transiently reversed, stopped for a few seconds, and then disappeared suddenly (track marked by an asterisk).

(E) Velocity histogram for fast forward movements of faint GFP-Myo10 particles (531 measurements from 65 filopodia) labeled with the mean ± standard deviation.
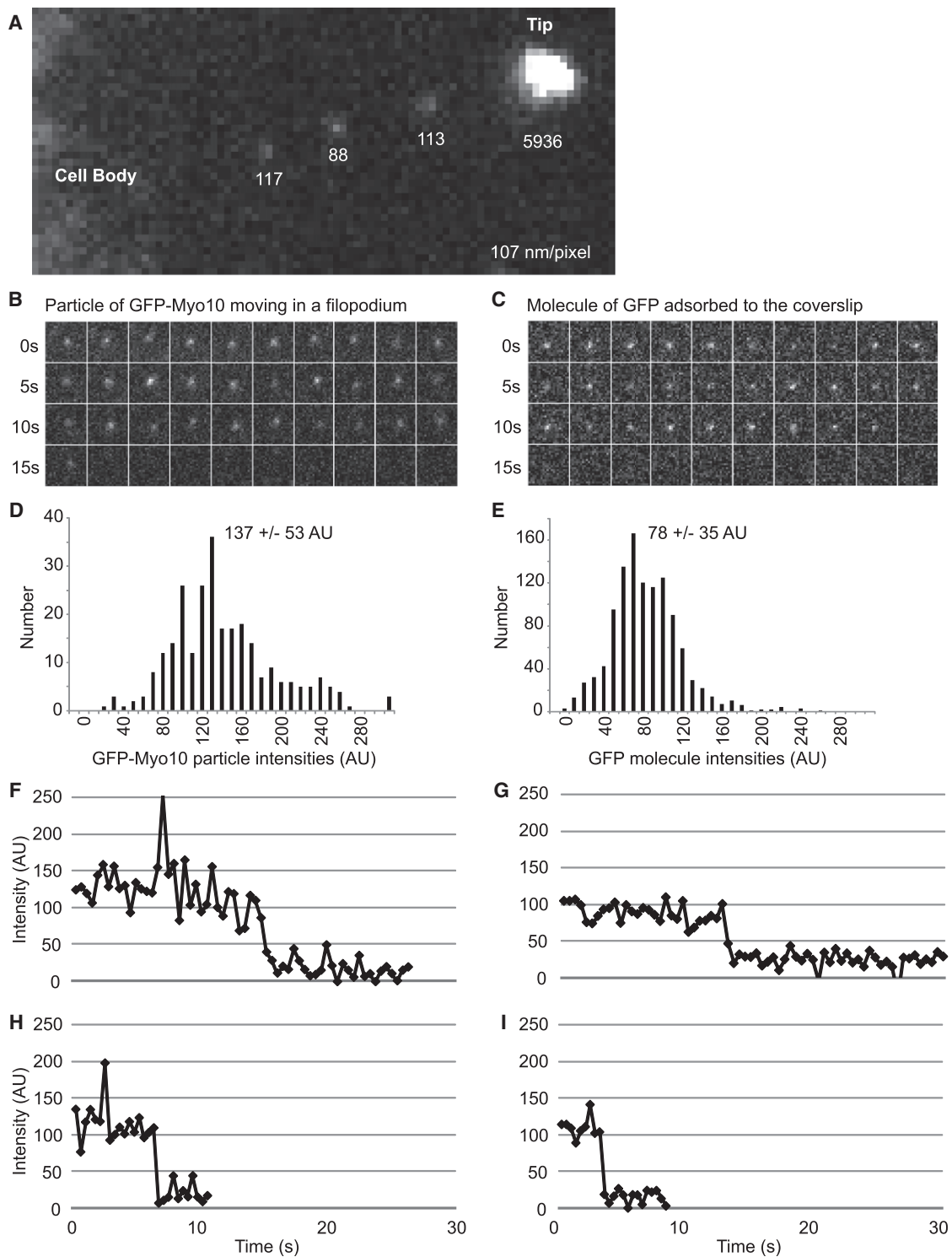
Figure 2. Faint Particles of GFP-Myo10 Exhibit Characteristics of Single Molecules

(A) High-magnification TIRF image of a filopodium showing a bright punctum of GFP-Myo10 at the tip and the diffraction-limited nature of three faint particles within the filopodial shaft. The numbers indicate the background-corrected, integrated intensity for each spot.

(B) Images from Kymotracker showing a single faint particle of GFP-Myo10 as it moved rapidly toward the tip of a filopodium and an apparent bleaching event at ∼15 s.

(C) Images from Kymotracker showing a single molecule of GFP adsorbed to a coverslip and an apparent bleaching event.

(D) Intensity histogram of faint particles of GFP-Myo10 moving rapidly forward in filopodia (268 measurements from 8 filopodia).

(E) Intensity histogram of single molecules of GFP adsorbed to coverslip surface (1124 measurements). Histograms are labeled with the mean ± standard deviation.

(F and H) Intensity-versus-time plots from Kymotracker for single particles of GFP-Myo10 that underwent apparent bleaching events as they moved rapidly forward in filopodia. Note that each particle disappeared in a single step rather than gradually fading away.

(G and I) Intensity-versus-time plots from Kymotracker for single molecules of GFP adsorbed on a coverslip.

A GFP-Myo10-headless
8.7μm

B GFP-Myo10-HMM
9.4μm

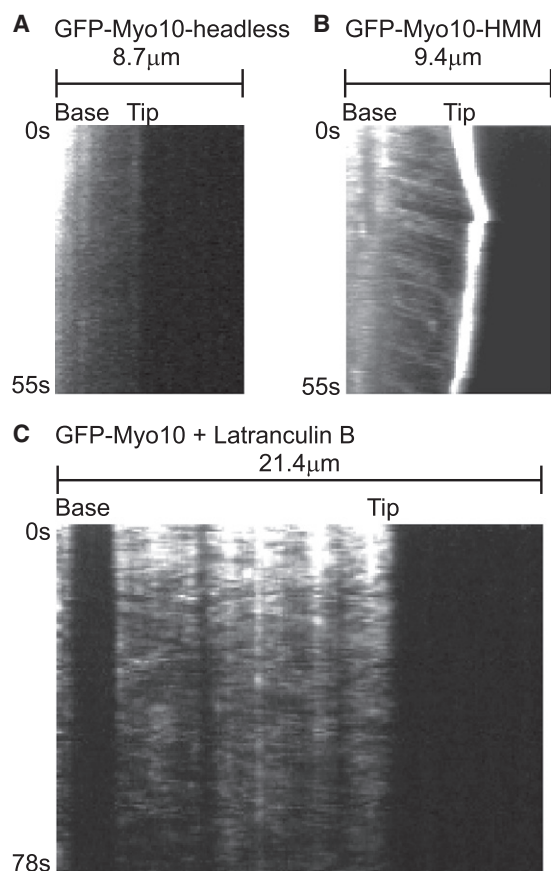**C** GFP-Myo10 + Latrunculin B
21.4μm

Figure 3. Fast Forward Movements Require the Myo10 Motor Domain and Are Inhibited by Latrunculin B

(A) Kymograph from TIRF imaging of GFP-Myo10-headless in a filopodium. This construct lacks most of the Myo10 motor domain and does not localize to filopodial tips or exhibit obvious fast forward movements.

(B) Kymograph from TIRF imaging of GFP-Myo10-HMM. GFP-Myo10-HMM is sufficient for tip localization and faint particles of it undergo fast forward movements.

(C) Kymograph showing that fast forward movements of GFP-Myo10 are blocked by latrunculin B. Cells were treated with 1 μM latrunculin B for ~10 min to depolymerize actin filaments and the remaining, substrate-attached filopodia were imaged by TIRF.

of retraction fibers (Figure 1C). Because Myo10 particles exhibited the same kinds of motility in both forms of slender extension and both forms of extension contained filopodial markers such as F-actin and the actin bundling protein, fascin (Figure S2), we follow the convention in Svitkina et al. and refer to these slender extensions collectively as filopodia [22].

Faint Myo10 Particles Have Single-Molecule Characteristics

We next investigated whether the faint particles detected by TIRF exhibited properties expected of single molecules [15, 21]. High-magnification views show that the faint particles moving within filopodia are approximately the size expected for a diffraction-limited spot (~0.2 μm at half maximum intensity), whereas the bright puncta at filopodial tips are generally much larger (Figure 2). Manual measurements indicated that the faint particles had integrated intensities of ~100 arbitrary units (AU), which is approximately 1/10th to 1/100th the intensity of a typical tip punctum. To facilitate particle tracking and quantification, we wrote a program called Kymotracker,

which utilizes the position and time coordinates from a line on a kymograph to semiautomatically track a particle and measure its intensity through time. As can be seen from the Kymotracker images of a faint particle of GFP-Myo10 as it moves along a filopodium, the faint particles appear diffraction limited and exhibit relatively constant intensities as they move (Figure 2B). In some cases, a particle that had been tracked through several frames disappeared suddenly, as would be expected for photobleaching of a single GFP. With Kymotracker, the average intensity of the faint particles of GFP-Myo10 in filopodia was found to be 137 ± 53 AU. The intensities of single GFP molecules adsorbed to coverslips and imaged under the same illumination and exposure conditions had a similar magnitude and an overlapping distribution (78 ± 35 AU) (Figures 2D and 2E), although it should be noted that the pure GFP was imaged in TBS rather than cytoplasm. Plots of intensity versus time revealed apparent stepwise bleaching events both for pure GFP on coverslips and for the faint particles moving within filopodia (Figures 2F–2I). Together these experiments demonstrate that the TIRF system used here can detect single molecules of pure GFP and that the faint particles of GFP-Myo10 detected in living cells correspond to single molecules or small oligomers.

Particle Movements Require the Myo10 Motor and Actin

To investigate the mechanisms responsible for the rapid movement of Myo10, we utilized a panel of Myo10 deletion constructs. No rapid particle movements and no tip localization were detected in HeLa cells transfected with GFP-Myo10-headless, a naturally occurring form of Myo10 that lacks most of the motor domain and thus lacks motor activity [9] (Figure 3A). In addition, no tracks representing fast forward movement were detected with a full-length Myo10 construct containing a point mutation in its motor domain that corresponds to a weak actin-binding mutation in other myosins [23] (GFP-Myo10-E456K; Figure S3). GFP-Myo10-HMM, which consists of the Myo10 motor, neck, and predicted coiled coil, did undergo rapid particle movements similar to those of full-length Myo10 (Figure 3B). This suggests that a dimerized Myo10 head-neck domain is sufficient for fast forward movements. Because systematic analysis of deletion constructs indicated that a forced-dimer construct consisting of the Myo10 head, neck, and first 34 amino acids of the "coiled coil" fused to a GCN4 dimerization domain was the minimal construct able to clearly localize to filopodial tips, we imaged the forced dimer by TIRF and found that it was also capable of fast forward movements in filopodia (Figure S3). Together these experiments indicate that rapid movements of faint particles in filopodia require Myo10 motor activity and that dimerization of the head-neck region is sufficient for fast forward movement and tip localization.

To test whether the fast forward movements are dependent on actin, cells were treated with 1 μM latrunculin B to depolymerize actin filaments. As expected, this triggered the collapse of filopodia that were not attached to the substrate (not shown). Although latrunculin did not induce collapse of most substrate-attached filopodia, it did cause the loss or spreading of the bright puncta of GFP-Myo10 normally present at their tips (Figure 3C). Most importantly, fast forward movements of GFP-Myo10 were not detected after treatment with latrunculin B, indicating that the fast forward movements are indeed dependent on F-actin. Treatment of cells with 5 μM nocodazole did not block fast forward movements of GFP-Myo10 (data not shown).
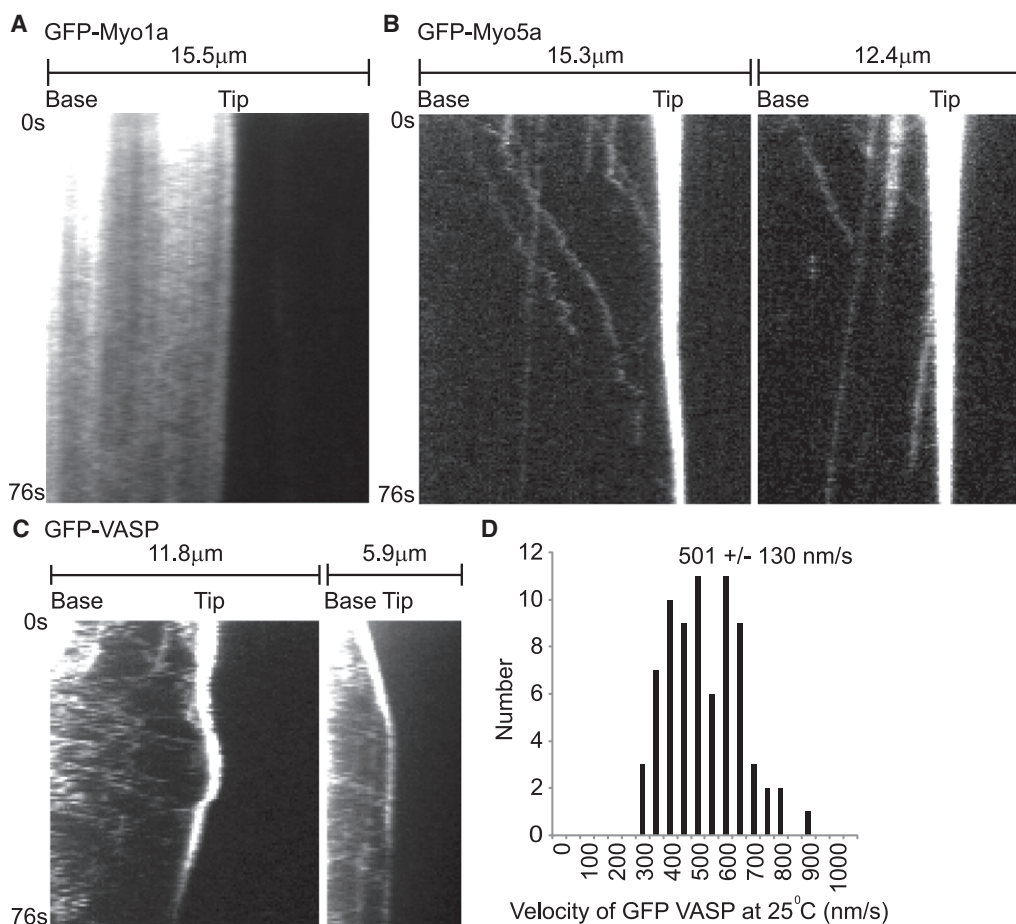
Figure 4. Faint Particles of GFP-Myo5a and GFP-VASP also Move Forward in the Filopodia of Living Cells

(A) Kymographs from TIRF imaging of GFP-Myo1a in filopodia. GFP-Myo1a did not localize to the tips of filopodia and no tracks corresponding to rapid forward movement were detected.

(B) Kymographs from TIRF imaging of GFP-Myo5a in filopodia. Note that several faint particles of GFP-Myo5a moved rapidly toward the tip while others moved slowly rearward.

(C) Kymographs of filopodia from HeLa cells transfected with GFP-VASP and imaged with standard TIRF imaging conditions. Note that GFP-VASP localizes to filopodial tips and generates faint tracks corresponding to rapid forward movement. For GFP-Myo1a and GFP-Myo5a data, frames were acquired at ~2.3 frames per second, whereas the VASP data was acquired at ~1.6 frames per second. This resulted in fewer acquired frames and thus shorter kymographs for the VASP data, despite identical 76 s durations.

(D) Velocity histogram for fast forward movements of GFP-VASP particles labeled with the mean ± standard deviation.

Faint Particles of GFP-Myo5a Undergo Similar Movements

To test whether other myosins were capable of similar movements within filopodia, we imaged HeLa cells transfected with GFP-Myo1a (brush border myosin I), a monomeric myosin that is nonprocessive and localizes to microvilli [24]. TIRF showed that GFP-Myo1a yielded a diffuse localization along the filopodia with no obvious enrichment at the filopodial tip (Figure 4A). Importantly, GFP-Myo1a did not undergo detectable fast forward movements in filopodia, indicating that not all myosins are capable of rapid directed movements in filopodia. We also tested GFP-Myo5a [25], an intensively studied dimeric myosin that is processive and functions in organelle transport [26] and filopodial dynamics [27]. Interestingly, GFP-Myo5a was enriched at the tips of filopodia, and faint particles of GFP-Myo5a generated clear tracks corresponding to rapid forward movement (Figure 4B). However, the GFP-Myo5a particles moved at only ~251 ± 121 nm/s (59 measurements from 22 filopodia), significantly (p = 0.035) slower than the ~578 nm/s observed for GFP-Myo10. The velocity of the GFP-Myo5a particles is very similar to the 270–330 nm/s

reported for individual molecules of a dimeric Myo5a construct moving on actin bundles in vitro [20]. It is therefore likely that the rapid and directed movements of GFP-Myo5a detected here correspond to the visualization of individual Myo5a molecules moving along the actin filaments of living cells. As with GFP-Myo10, faint particles of GFP-Myo5a sometimes moved slowly rearward at the retrograde flow rate of ~10–20 nm/s (Figure 4B). This observation provides direct evidence that Myo5a can indeed undergo retrograde flow, as recently hypothesized [28].

Conclusions

The TIRF experiments reported here reveal a novel form of long-range motility driven by myosin motors at or near the single-molecule level. The fast movements require Myo10 motor activity and actin filaments, but not the Myo10 tail. Together, these results strongly support the hypothesis that Myo10 molecules use their barbed-end motor activity to move forward along filopodial actin filaments (see model illustrated in Movie S5). The faint particles detected with

TIRF exhibit a size, intensity range, and bleaching behavior consistent with imaging at the single-molecule level. It is not yet clear, however, whether these particles correspond to monomers, dimers, or small oligomers of Myo10. Several factors contribute to this uncertainty, including the relatively high and variable background fluorescence present in living cells, variable levels of protein expression, the nonideal behavior of GFP as a fluorophore, and variations in the Z-axis position of the filopodium or molecules within it. It should also be noted that although we can clearly detect the movements of some particles, we cannot guarantee unambiguous detection of every GFP-Myo10 molecule in a filopodium. Despite these limits, the combination of TIRF and GFP tagging used here provides a powerful strategy for imaging the movements of motor proteins and their cargos at or near the single-molecule level in living cells.

In addition to exhibiting a novel form of rapid, long-range motility in filopodia, Myo10 also has potent filopodia-promoting activity. Our previous work indicates that Myo10's ability to induce numerous filopodia requires (1) elements within the Myo10 tail and (2) the ability to localize to filopodial tips [10]. We now find that only Myo10 constructs capable of moving rapidly forward in filopodia are able to localize to filopodial tips, so the novel form of motility reported here is likely to underlie both tip localization and filopodia promotion. Although the precise mechanism(s) by which Myo10 promotes filopodia are not yet clear, it could act by initiating filopodia, by transporting cargos that facilitate filopodia formation, by functioning as part of a mobile tip complex, or by some combination of these or other mechanisms [9, 10, 14].

As a motor that moves rapidly along filopodia, Myo10 clearly transports itself to the filopodial tip, but it may also be responsible for the transport of other specific molecular cargos, such as VASP [29]. Indeed, preliminary experiments indicate that faint particles of GFP-VASP exhibit fast forward movements in filopodia very similar to those of Myo10 (Figures 4C and 4D). A major goal for the future will be to test for cotransport at the single-molecule level and to determine whether Myo10 is required for transport of this and other cargos. It will also be interesting to determine whether Myo3a or Myo15a, myosins that localize to the tips of stereocilia and are necessary for hearing, undergo similar forms of movement [28, 30, 31]. In addition to revealing a novel form of motility, this work also suggests that motor proteins may power many as yet undetected movements at the single-molecule level.

Supplemental Data

Acknowledgments

References

1. Hu, K., Ji, L., Applegate, K.T., Danuser, G., and Waterman-Storer, C.M. (2007). Differential transmission of actin motion within focal adhesions. Science 315, 111–115.
2. Lidke, D.S., Lidke, K.A., Rieger, B., Jovin, T.M., and Arndt-Jovin, D.J. (2005). Reaching out for signals: filopodia sense EGF and respond by directed retrograde transport of activated receptors. J. Cell Biol. 170, 619–626.
3. Sherer, N.M., Lehmann, M.J., Jimenez-Soto, L.F., Horensavitz, C., Pypaert, M., and Mothes, W. (2007). Retroviruses can establish filopodial bridges for efficient cell-to-cell transmission. Nat. Cell Biol. 9, 310–315.
4. Berg, J.S., and Cheney, R.E. (2002). Myosin-X is an unconventional myosin that undergoes intrafilopodial motility. Nat. Cell Biol. 4, 246–250.
5. Mattila, P.K., and Lappalainen, P. (2008). Filopodia: Molecular architecture and cellular functions. Nat. Rev. Mol. Cell Biol. 9, 446–454.
6. Wood, W., and Martin, P. (2002). Structures in focus—filopodia. Int. J. Biochem. Cell Biol. 34, 726–730.
7. Albrecht-Buehler, G., and Goldman, R.D. (1976). Microspike-mediated particle transport towards the cell body during early spreading of 3T3 cells. Exp. Cell Res. 97, 329–339.
8. Medeiros, N.A., Burnette, D.T., and Forscher, P. (2006). Myosin II functions in actin-bundle turnover in neuronal growth cones. Nat. Cell Biol. 8, 215–226.
9. Sousa, A.D., and Cheney, R.E. (2005). Myosin-X: A molecular motor at the cell's fingertips. Trends Cell Biol. 15, 533–539.
10. Bohil, A.B., Robertson, B.W., and Cheney, R.E. (2006). Myosin-X is a molecular motor that functions in filopodia formation. Proc. Natl. Acad. Sci. USA 103, 12411–12416.
11. Rogers, M.S., and Strehler, E.E. (2001). The tumor-sensitive calmodulin-like protein is a specific light chain of human unconventional myosin X. J. Biol. Chem. 276, 12182–12189.
12. Berg, J.S., Derfler, B.H., Pennisi, C.M., Corey, D.P., and Cheney, R.E. (2000). Myosin-X, a novel myosin with pleckstrin homology domains, associates with regions of dynamic actin. J. Cell Sci. 113, 3439–3451.
13. Knight, P.J., Thirumurugan, K., Yu, Y., Wang, F., Kalverda, A.P., Stafford, W.F., 3rd, Sellers, J.R., and Peckham, M. (2005). The predicted coiled-coil domain of myosin 10 forms a novel elongated domain that lengthens the head. J. Biol. Chem. 280, 34702–34708.
14. Tokuo, H., Mabuchi, K., and Ikebe, M. (2007). The motor activity of myosin-X promotes actin fiber convergence at the cell periphery to initiate filopodia formation. J. Cell Biol. 179, 229–238.
15. Mashanov, G.I., Tacon, D., Peckham, M., and Molloy, J.E. (2004). The spatial and temporal dynamics of pleckstrin homology domain binding at the plasma membrane measured by imaging single molecules in live mouse myoblasts. J. Biol. Chem. 279, 15274–15280.
16. Weber, K.L., Sokac, A.M., Berg, J.S., Cheney, R.E., and Bement, W.M. (2004). A microtubule-binding myosin required for nuclear anchoring and spindle assembly. Nature 431, 325–329.
17. Zhang, H., Berg, J.S., Li, Z., Wang, Y., Lang, P., Sousa, A.D., Bhaskar, A., Cheney, R.E., and Stromblad, S. (2004). Myosin-X provides a motor-based link between integrins and the cytoskeleton. Nat. Cell Biol. 6, 523–531.
18. Kovacs, M., Wang, F., and Sellers, J.R. (2005). Mechanism of action of myosin X, a membrane-associated molecular motor. J. Biol. Chem. 280, 15071–15083.
19. Homma, K., and Ikebe, M. (2005). Myosin X is a high duty ratio motor. J. Biol. Chem. 280, 29381–29391.
20. Nagy, S., Ricca, B.L., Norstrom, M.F., Courson, D.S., Brawley, C.M., Smithback, P.A., and Rock, R.S. (2008). A myosin motor that selects bundled actin for motility. Proc. Natl. Acad. Sci. USA 105, 9616–9620.
21. Pierce, D.W., Hom-Booher, N., and Vale, R.D. (1997). Imaging individual green fluorescent proteins. Nature 388, 338.
22. Svitkina, T.M., Bulanova, E.A., Chaga, O.Y., Vignjevic, D.M., Kojima, S., Vasiliev, J.M., and Borisy, G.G. (2003). Mechanism of filopodia initiation by reorganization of a dendritic network. J. Cell Biol. 160, 409–421.
23. Friedman, A.L., Geeves, M.A., Manstein, D.J., and Spudich, J.A. (1998). Kinetic characterization of myosin head fragments with long-lived myosin.ATP states. Biochemistry 37, 9679–9687.
24. Tyska, M.J., and Mooseker, M.S. (2002). MYO1A (brush border myosin I) dynamics in the brush border of LLC-PK1–CL4 cells. Biophys. J. 82, 1869–1883.

25. Wu, X., Wang, F., Rao, K., Sellers, J.R., and Hammer, J.A., 3rd. (2002). Rab27a is an essential component of melanosome receptor for myosin Va. Mol. Biol. Cell *13*, 1735–1749.

26. Trybus, K.M. (2008). Myosin V from head to tail. Cell. Mol. Life Sci. *65*, 1378–1389.

27. Wang, F.S., Wolenski, J.S., Cheney, R.E., Mooseker, M.S., and Jay, D.G. (1996). Function of myosin-V in filopodial extension of neuronal growth cones. Science *273*, 660–663.

28. Liu, J., Taylor, D.W., Krementsova, E.B., Trybus, K.M., and Taylor, K.A. (2006). Three-dimensional structure of the myosin V inhibited state by cryoelectron tomography. Nature *442*, 208–211.

29. Tokuo, H., and Ikebe, M. (2004). Myosin X transports Mena/VASP to the tip of filopodia. Biochem. Biophys. Res. Commun. *319*, 214–220.

30. Schneider, M.E., Dose, A.C., Salles, F.T., Chang, W., Erickson, F.L., Burnside, B., and Kachar, B. (2006). A new compartment at stereocilia tips defined by spatial and temporal patterns of myosin IIIa expression. J. Neurosci. *26*, 10243–10252.

31. Belyantseva, I.A., Boger, E.T., Naz, S., Frolenkov, G.I., Sellers, J.R., Ahmed, Z.M., Griffith, A.J., and Friedman, T.B. (2005). Myosin-XVa is required for tip localization of whirlin and differential elongation of hair-cell stereocilia. Nat. Cell Biol. *7*, 148–156.